Electronic Supporting Information (ESI)

Interlayer hydrogen bonding directed magnetic properties for different number of waters intercalated structural heterometallic phosphates based on paddlewheel units $Ru_2(PO_4)_4^{6-}$

Xiangxian Xue, Tuo Ding Pei Zhang, Jianhui Yang and Bin Liu*

Key Laboratory of Synthetic and Natural Functional Molecule of the Ministry of Education, Shaanxi Key Laboratory of Physico-Inorganic Chemistry, College of Chemistry & Materials Science, Northwest University, Xi'an 710127, P. R. China

Table S1. Crystallographic data and structure refinement details for **1**·$10H_2O$ and **1**·$4H_2O$.

Compound	**1**·$10H_2O$	**1**·$4H_2O$
Empirical formula	$H_{44}Mn_3Ru_2P_4O_{38}$	$H_{32}Mn_3Ru_2P_4O_{32}$
M_r	1143.19	1035.09
Crystal system	Orthorhombic	Monoclinic
Space group	*Pbca*	$P2_1/c$
a [Å]	16.1522(18)	7.5776(16)
b [Å]	9.8495(11)	9.922(2)
c [Å]	19.642(2)	19.421(4)
α [°]	90	90
β [°]	90	111.735(7)
γ [°]	90	90
V [Å^3]	3124.8(6)	1356.4(5)
Z	4	2
ρ_{calcd} [g·cm^{-3}]	2.430	2.534
μ [mm^{-1}]	2.463	2.808
F(000)	2284	1022
GOF on F^2	1.087	1.049
Reflections collected (total/unique)	15923/2926	6417/2378
$R_{(int)}$	0.048	0.036
R_1, wR_2 [$I>2\sigma(I)$][a]	0.0468, 0.1455	0.0420, 0.1226
$(\Delta\rho)_{max}$, $(\Delta\rho)_{min}$ [e/Å^3]	1.178, -1.235	3.204, -0.900

[a] $R_1 = \Sigma||F_o| - |F_c||/\Sigma|F_o|$; $wR_2 = [\Sigma w(F_o^2 - F_c^2)^2/\Sigma w(F_o^2)^2]^{1/2}$

* Corresponding author. Tel./fax: +86-029-88302604.

E-mail address: liubin@nwu.edu.cn (B. Liu).

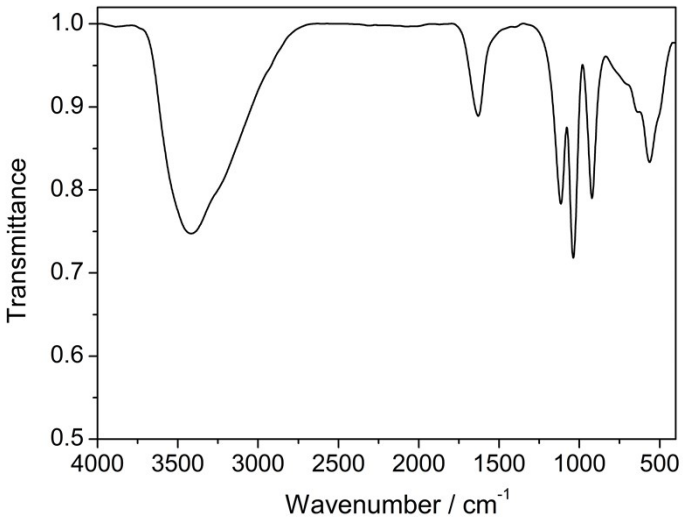

Fig. S1 IR spectrum of compound **1**·10H_2O.

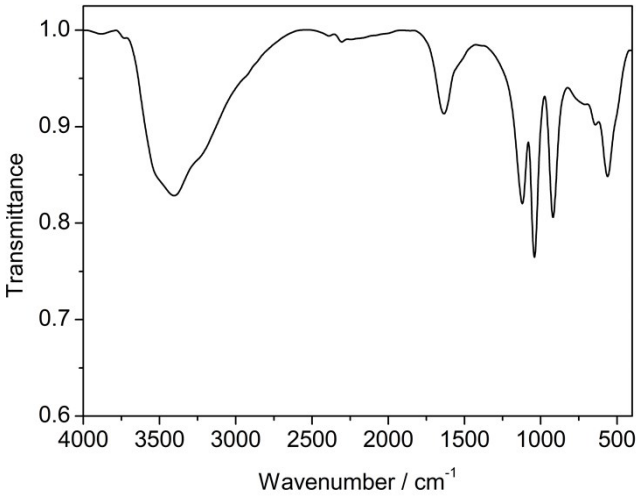

Fig. S2 IR spectra of compound **1**·4H_2O.

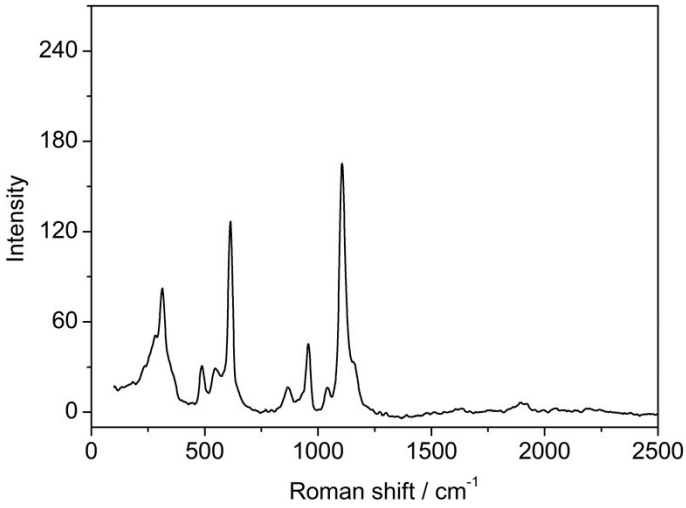

Fig. 3 Raman spectrum of compound **1**·10H_2O in solid form recorded at 300 K with excitation wavelengths of 532 nm.

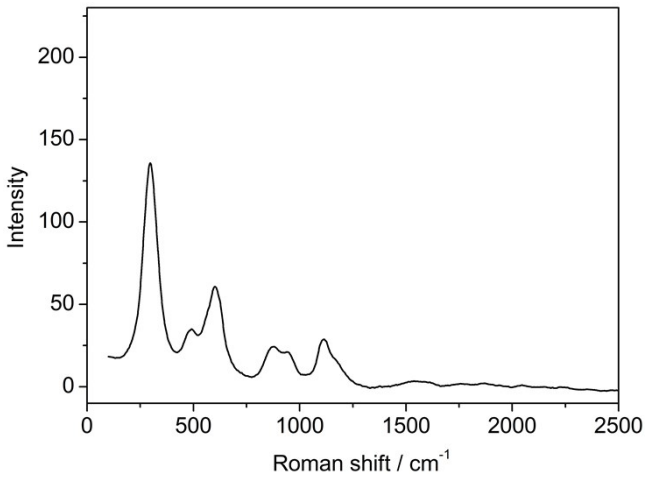

Fig. 4 Raman spectrum of compound **1**·$4H_2O$ in solid form recorded at 300 K with excitation wavelengths of 532 nm.

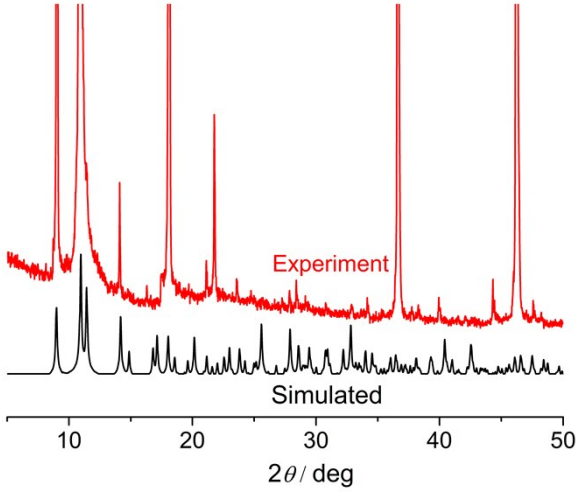

Fig. S5 Comparison of XRPD patterns of the simulated pattern from the single-crystal structure determination and as-synthesized perfect crystals of compound **1**·$10H_2O$.

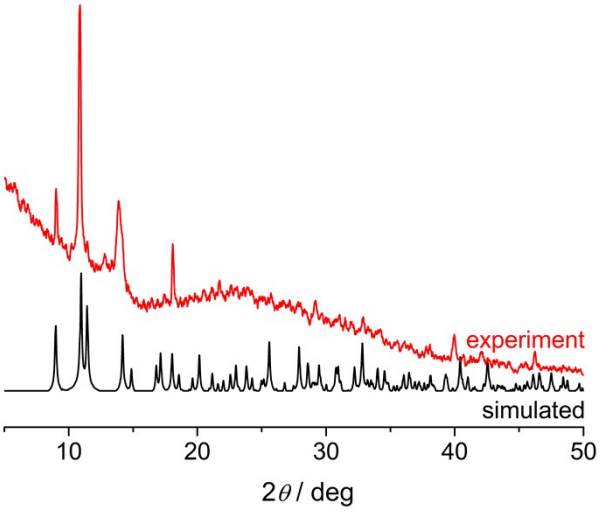

Fig. S6 Comparison of XRPD patterns of the simulated pattern from the single-crystal structure determination and as-synthesized powder samples of compound **1**·$10H_2O$.

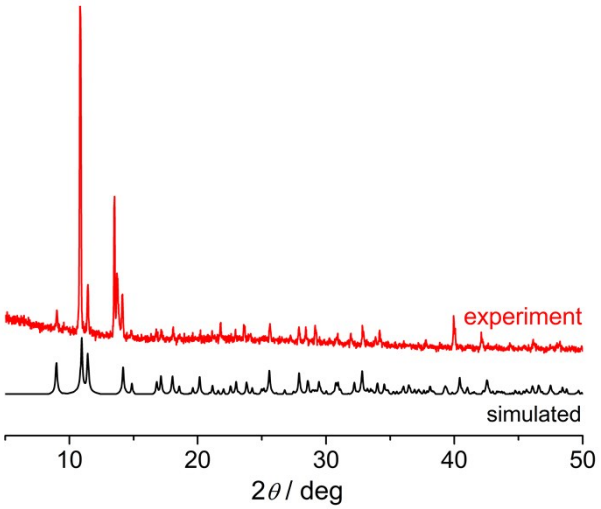

Fig. S7 Comparison of XRPD patterns of the simulated pattern from the single-crystal structure determination of compound **1**·$10H_2O$ and the powder samples synthesized by $Mn(CH_3CO_2)_2$.

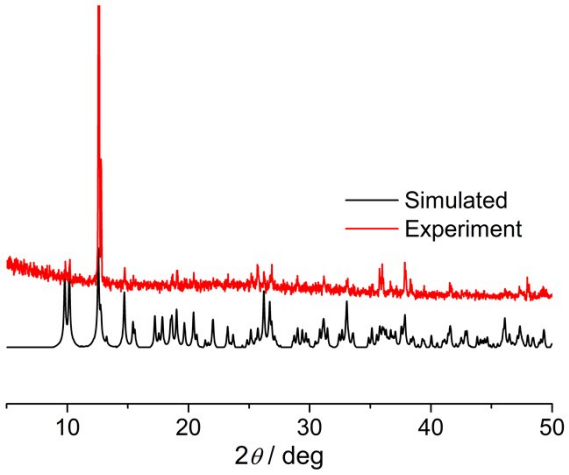

Fig. S8 Comparison of XRPD patterns of the simulated pattern from the single-crystal structure determination and as-synthesized product of compound **1**·$4H_2O$.

Compared with compound **1**·$4H_2O$, the PXRD patterns of both perfect crystals and powders of compound **1**·$10H_2O$ showed that the agreement between simulated and experiment is not very good. The perfect crystals exhibiting fewer diffraction peaks (as shown in Figure S5) may be due to the preferential orientation of crystalline grain arrangement, however, the slight disagreement of PXRD for powder samples could attributed the crystal dehydration, and it is also consistent with the TG plot (Figure S9), in which the crystallization water is very easily lost even at room temperature. To summarise, the detailed experiments show that the alkaline strength of the presence anions plays the key role in directing different number of lattice waters intercalated structures, and pH directs its final pure phase.

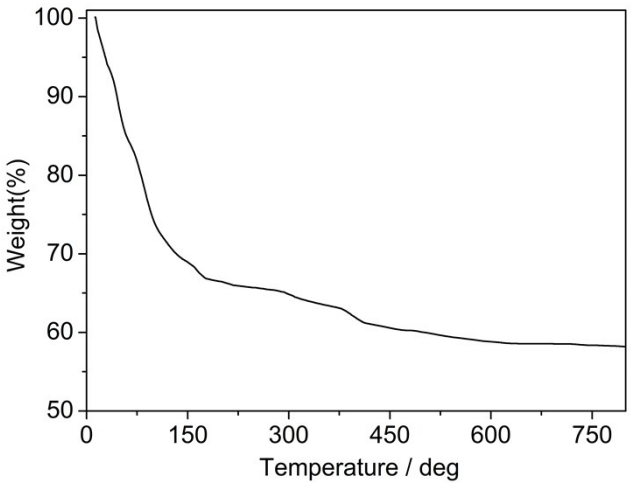

Fig. S9 TG curve of compound **1**·10H_2O.

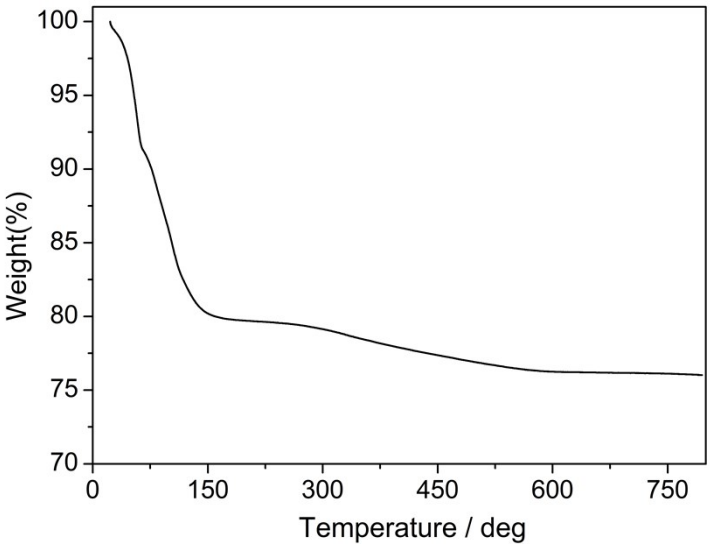

Fig. S10 TG curve of compound **1**·4H_2O.

Fig. S11 Crystals of compound **1**·10H_2O

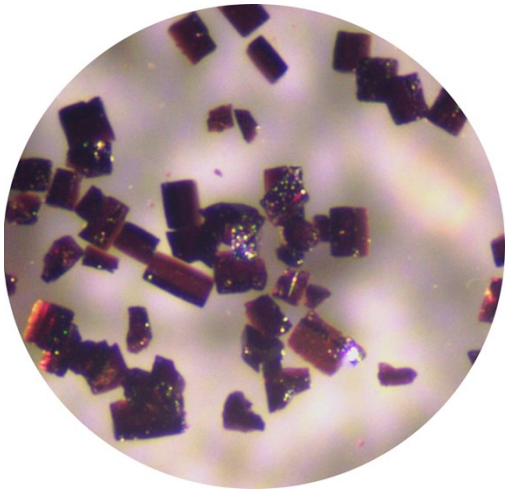

Fig. S12 Crystals of compound **1**·4H_2O

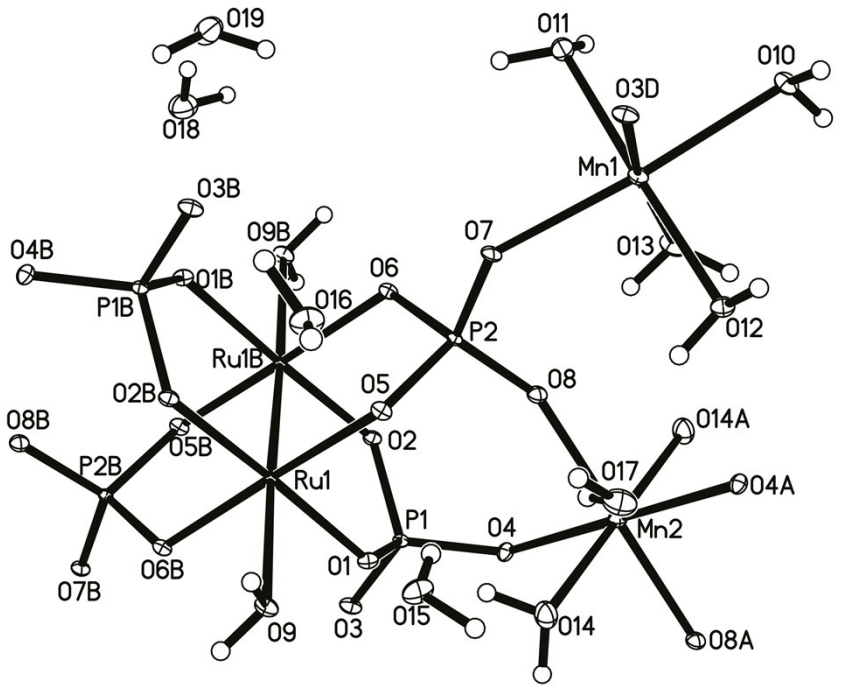

Fig. S13 ORTEP representation (20% thermal probability ellipsoids) of the crystal structure of compound **1**·10H_2O **(**H atoms are omitted for clarity**)**.

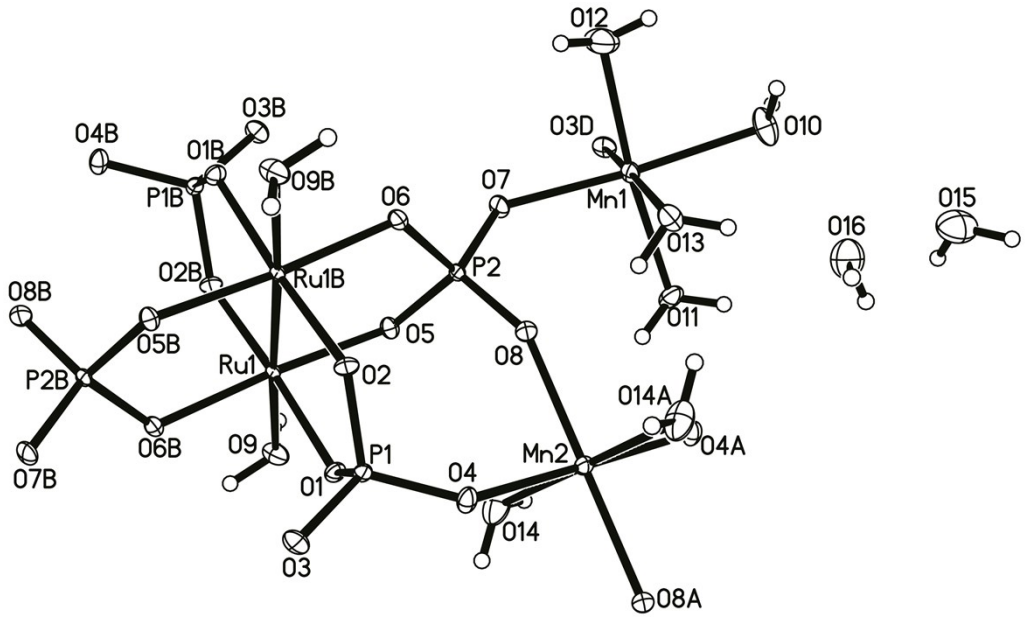

Fig. S14 ORTEP representation (20% thermal probability ellipsoids) of the crystal structure of compound **1**·4H_2O.

Table S2. The bond distances (Å) of **1**·10H_2O and **1**·4H_2O.

	1·10H_2O	**1**·4H_2O
Ru(1)–Ru(1b)	2.3508(5)	2.3377(7)
Ru(1)–O(1)	1.974(3)	1.972(4)
Ru(1)–O(5)	1.995(3)	1.994(4)
Ru(1)–O(2b)	1.980(3)	1.958(4)
Ru(1)–O(6b)	1.994(3)	1.983(4)
Ru(1)–O(9)	2.316(3)	2.330(5)
Mn(1)–O(3d)	2.100(3)	2.083(4)
Mn(1)–O(7)	2.166(3)	2.127(4)
Mn(1)–O(10)	2.169(4)	2.210(5)
Mn(1)–O(11)	2.166(3)	2.193(5)
Mn(1)–O(12)	2.169(3)	2.188(6)
Mn(1)–O(13)	2.305(4)	2.246(4)
Mn(2)–O(4)	2.190(3)	2.203(4)
Mn(2)–O(8)	2.138(3)	2.160(4)
Mn(2)–O(4a)	2.190(3)	2.203(4)
Mn(2)–O(8a)	2.138(3)	2.160(4)
Mn(2)–O(14)	2.223(5)	2.179(5)
Mn(2)–O(14a)	2.223(5)	2.179(5)
P(1)–O(1)	1.570(3)	1.581(4)
P(1)–O(2)	1.570(3)	1.570(4)
P(1)–O(3)	1.516(4)	1.510(4)
P(1)–O(4)	1.517(3)	1.514(4)
P(2)–O(5)	1.574(3)	1.572(4)
P(2)–O(6)	1.584(3)	1.577(4)
P(2)–O(7)	1.518(3)	1.513(4)
P(2)–O(8)	1.508(3)	1.511(4)

Symmetry codes: a 1-x,1-y,1-z; b 1-x,2-y,1-z; c x,3/2-y,-1/2+z; d x,3/2-y,1/2+z.

Table S3. The bond angles (˚) of compounds **1**·10H_2O and **1**·4H_2O.

	1·10H_2O	**1**·4H_2O
Ru(1b)–Ru(1)–O(1)	91.88(9)	93.06(12)
Ru(1b)–Ru(1)–O(5)	92.12(9)	91.10(12)
Ru(1b)–Ru(1)–O(2b)	92.69(9)	91.95(12)
Ru(1b)–Ru(1)–O(6b)	92.24(9)	93.54(12)
Ru(1b)–Ru(1)–O(9)	177.26(11)	175.73(10)
O(1)–Ru(1)–O(5)	89.98(13)	89.45(16)

O(1)–Ru(1)–O(9)	85.39(14)	88.82(16)
O(1)–Ru(1)–O(2b)	175.39(13)	174.76(17)
O(1)–Ru(1)–O(6b)	91.28(12)	88.76(16)
O(5)–Ru(1)–O(9)	87.97(13)	85.08(16)
O(2b)–Ru(1)–O(5)	89.26(13)	91.99(16)
O(5)–Ru(1)–O(6b)	175.43(13)	175.11(17)
O(2b)–Ru(1)–O(9)	90.04(14)	86.28(16)
O(6b)–Ru(1)–O(9)	87.75(13)	90.33(16)
O(2b)–Ru(1)–O(6b)	89.13(12)	89.40(16)
Ru(1)–O(1)–P(1)	123.95(18)	123.1(2)
Ru(1b)–O(2)–P(1)	123.04(19)	124.8(2)
Ru(1)–O(5)–P(2)	120.71(18)	122.8(2)
Ru(1b)–O(6)–P(2)	120.85(18)	120.6(2)
O(7)–Mn(1)–O(10)	171.73(12)	168.96(19)
O(7)–Mn(1)–O(11)	88.18(13)	97.33(17)
O(7)–Mn(1)–O(12)	93.72(12)	87.4(2)
O(7)–Mn(1)–O(13)	91.55(13)	88.36(15)
O(3d)–Mn(1)–O(7)	93.94(13)	94.11(16)
O(10)–Mn(1)–O(11)	85.16(13)	89.59(18)
O(10)–Mn(1)–O(12)	92.87(13)	85.2(2)
O(10)–Mn(1)–O(13)	84.12(13)	83.42(18)
O(3d)–Mn(1)–O(10)	91.46(13)	94.94(18)
O(11)–Mn(1)–O(12)	177.92(13)	173.67(19)
O(11)–Mn(1)–O(13)	94.66(13)	86.95(15)
O(3d)–Mn(1)–O(11)	94.35(14)	86.00(16)
O(12)–Mn(1)–O(13)	84.44(13)	88.95(19)
O(3d)–Mn(1)–O(12)	86.39(14)	97.95(19)
O(3d)–Mn(1)–O(13)	169.60(15)	172.77(17)
O(4)–Mn(2)–O(8)	90.68(11)	88.98(15)
O(4)–Mn(2)–O(14)	90.86(13)	87.30(18)
O(4)–Mn(2)–O(4a)	180.00	180.00
O(4)–Mn(2)–O(8a)	89.32(11)	91.02(15)
O(4)–Mn(2)–O(14a)	89.15(13)	92.70(18)
O(8)–Mn(2)–O(14)	90.11(14)	86.43(17)
O(4a)–Mn(2)–O(8)	89.32(11)	91.02(15)
O(8)–Mn(2)–O(8a)	180.00	180.00
O(8)–Mn(2)–O(14a)	89.89(14)	93.57(17)
O(4a)–Mn(2)–O(14)	89.15(13)	92.70(18)

O(8a)–Mn(2)–O(14)	89.89(14)	93.57(17)
O(14)–Mn(2)–O(14a)	180.00	180.00
O(4a)–Mn(2)–O(8a)	90.68(11)	88.98(15)
O(4a)–Mn(2)–O(14a)	90.86(13)	87.30(18)
O(8a)–Mn(2)–O(14a)	90.11(14)	86.43(17)
Mn(1)–O(7)–P(2)	130.53(18)	131.9(2)
Mn(1c)–O(3)–P(1)	142.5(2)	138.3(3)
Mn(2)–O(4)–P(1)	126.76(19)	132.0(2)
Mn(2)–O(8)–P(2)	155.8(2)	150.6(3)

Symmetry codes: a 1-x,1-y,1-z; b 1-x,2-y,1-z; c x,3/2-y,-1/2+z; d x,3/2-y,1/2+z.

Table S4. Hydrogen bonds O—H…O in compound **1**·10H_2O **(**gray: intralayer hydrogen bonds; blank: lattice water hydrogen bonds**)**.

	O—H (Å)	O—H…O (Å)	Symmetry codes
O9…O14	0.85	2.867(6)	7_555
O10…O5	0.85	2.806(5)	4_645
O12…O7	0.85	2.735(4)	4_645
O13…O8	0.85	2.790(5)	
O14…O1	0.85	2.854(6)	
O14…O9	0.85	2.867(6)	7_545
O9…O15	0.85	2.683(5)	7_555
O10…O19	0.85	2.918(5)	1_545
O11…O16	0.85	2.755(5)	6_555
O11…O19	0.85	2.995(5)	7_645
O12…O17	0.85	2.977(5)	
O15…O17	0.85	2.748(5)	
O16…O13	0.85	2.735(5)	4_655
O17…O15	0.85	2.748(5)	
O3…O19	0.85	2.728(5)	5_665
O19…O16	0.85	2.656(5)	6_555

Table S5. Hydrogen bonds O—H…O in compound **1**·4H_2O (gray: interlayer hydrogen bonds; yellow: directly connected hydrogen bonds; blank: lattice water hydrogen bonds)

	O—H (Å)	O—H…O (Å)	Symmetry codes
O9…O6	0.87	2.7776(6)	1_655
O10…O5	0.84	2.798(5)	2_646
O11…O7	0.88	2.830(5)	2_646
O11…O4	0.85	2.709(5)	3_666
O12…O9	0.86	2.920(7)	1_455
O13…O8	0.86	2.701(6)	

O14…O13	0.89	2.745(7)	1_655
O9…O15	0.87	2.795(7)	1_665
O12…O15	0.87	2.773(8)	2_556
O13…O16	0.87	2.698(7)	
O15…O11	0.87	2.752(8)	2_646
O16…O15	0.88	2.832(9)	
O16…O1	0.87	2.904(8)	3_766

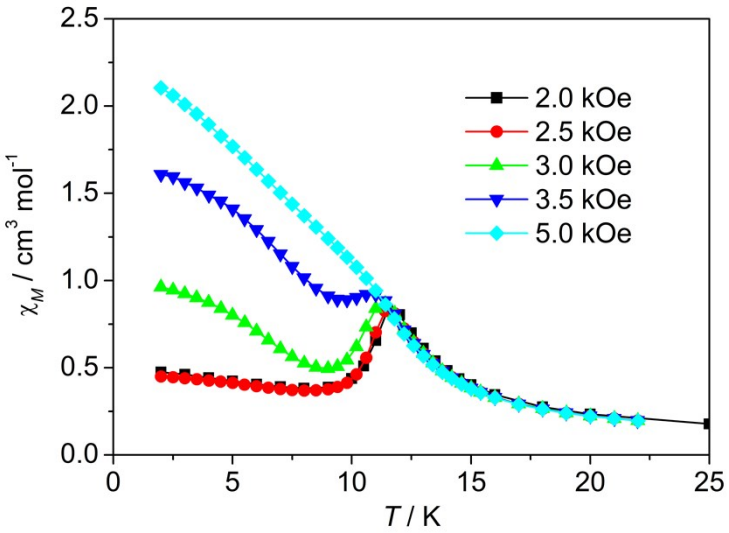

Fig. S15 χ_M in an applied field of 2.0, 2.5, 3.0, 3.5 and 5.0 kOe for compound **1**·4H_2O.

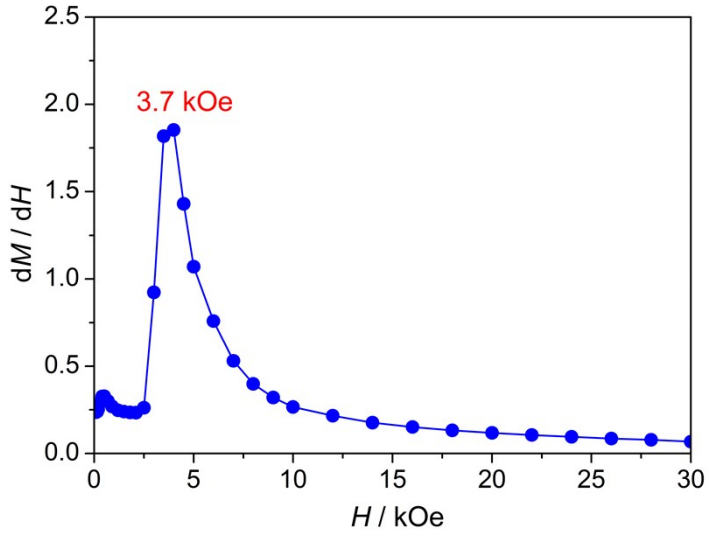

Fig. S16 The critical field determined by the dM/dH curve for compound **1**·4H_2O

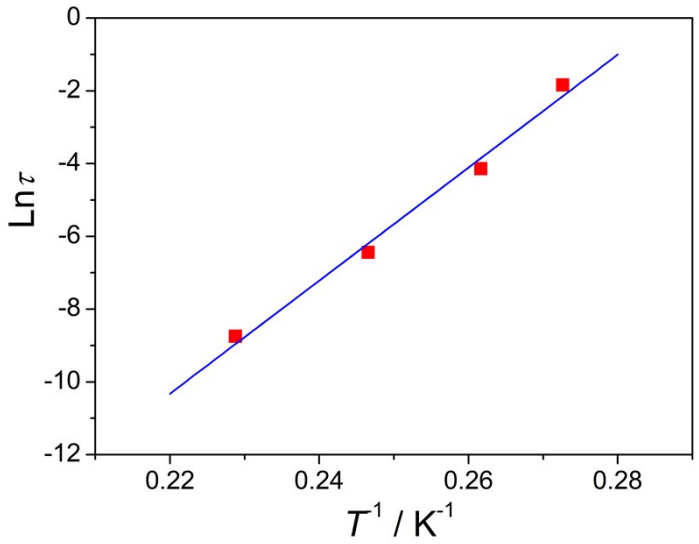

Fig. S17 lnτ *vs*. 1/*T* for **1**·10H_2O, the solid line is least-squares fit to the Arrhenius law (see text).

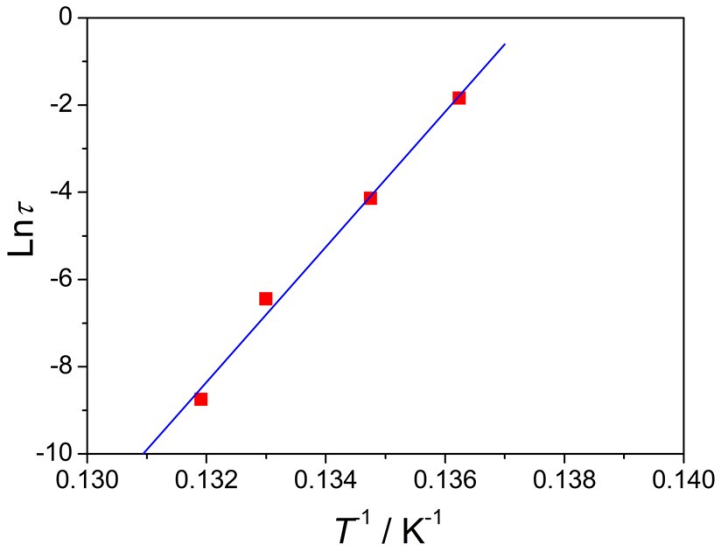

Fig. S18 lnτ *vs*. 1/*T* for **1**·4H_2O, the solid line is least-squares fit to the Arrhenius law (see text)